PAPER

Check for updates

Cannabis sativa biochar: characterization and preliminary application in plant growth and adsorption, and as an electrode material†

Maria Belen Ceretta, [iD] ‡[a] Sofia Antic Gorrazzi,‡[a] Sebastian D'Ippolito,[b] Julieta Mendieta,[b] Debora Nercessian[b] and Sebastian Bonanni [iD] *[a]

Cannabis sativa cultivation generates substantial solid residues and the growing demand for cannabis products, driven by the increasing number of countries and states legalizing its consumption, underscores the need for sustainable production practices that minimize environmental impact. Converting discarded cannabis biomass into biochar offers an eco-friendly waste management solution while producing a high-value product with diverse applications. Although the feasibility of these applications largely depends on the feedstock and pyrolysis conditions, studies on cannabis-derived biochar remain scarce. In this work, the impact of pyrolysis temperature on the physicochemical properties of *C. sativa* biochar is investigated and the performance of biochar produced at different temperatures as a soil amendment, electrode material and contaminant adsorbent is assessed.

Sustainability spotlight

This study explores sustainable practices in cannabis production by converting residual biomass into biochar. This approach aims to reduce the environmental impact of cannabis cultivation while offering innovative pathways for sustainable agricultural and industrial practices, in alignment with the principles of responsible production outlined in the UN Sustainable Development Goal (SDG) 12. The production of biochar from solid residues allows for the valorization of waste, due to the wide range of applications this material offers. In this work, we analyze some of these potential applications, including the use of biochar as a soil amendment to improve crop yield (also aligning with SDG 12), as an adsorbent to enhance water treatment processes (aligning with SDG 6), and as an electrode material to promote the use of environmentally friendly materials in energy technologies (SDG 7).

Introduction

In recent years, there has been a global trend toward the legalization of cannabis for both medicinal and recreational use. As a result, the global cannabis market is projected to grow at an annual rate of 21% until 2030.[1] Sustainable practices are essential to meet the demands of this rapidly expanding market while minimizing environmental impacts.

Cannabis production generates large amounts of solid residues.[2] Inflorescences are the primary component used for the production of cannabis derivatives whereas the remaining biomass, including stems, roots, and leaves, is typically discarded. Converting this residual biomass into biochar represents an environmentally and economically favourable strategy for managing these solid wastes.[3]

Biochar is a carbonous material obtained from the reductive pyrolysis of plant biomass or other organic waste. In this process, the materials are heated in an atmosphere with null or very low oxygen concentration, promoting physicochemical changes of plant tissues that result in a solid mainly composed of carbon in a highly stable mineral form. This avoids the release of CO_2 from plant tissues into the atmosphere, preventing greenhouse gas emissions and boosting carbon sequestration.[4] As a result, producing biochar from the unused parts of the cannabis plant would help to reduce the carbon footprint of the production process, reducing its environmental impact. Additionally, this offers an opportunity to upgrade plant waste by creating a high-value product with diverse applications.

Biochar has proven its versatility across multiple fields. Its addition into the soil improves the availability of N, P and Si, and generates appropriate microenvironments for the development of beneficial microorganisms for plants.[5–7] Besides,

[a]*Área Ingeniería de Interfases y Bioprocesos (IIBio), INTEMA. Av. Colon 10850, Mar del Plata (7600), Argentina. E-mail: sebastian.bonanni@mdp.edu.ar*

[b]*Biología de Cannabis, Instituto de Investigaciones Biológicas (IIB), Funes, Mar del Plata (7600), Argentina*

† Electronic supplementary information (ESI) available: TGA graphs, FTIR spectra, EDS analysis Raman spectra, fitting of ammonia adsorption isotherms with the Freundlich equation, additional physicochemical properties of biochar obtained at different temperatures, procedure for obtaining electrochemical kinetic constants and electrode capacitance and modelling of experimental cyclic voltammetries. See DOI: https://doi.org/10.1039/d4su00829d

‡ These authors contributed equally to the work.

biochar enhances water retention and regulates pH in the soil, contributing to boosting its structure and fertility.[8] For these reasons, it is widely applied as a soil amendment for enhancing crop yield.[9] Biochar has also been used in wastewater treatment for improving bacterial activity and pollutant removal efficiency[10] and as an adsorbent for diverse contaminants.[11–13] Furthermore, it has been tested as an electrode material in fuel cells, microbial fuel cells and other bioelectrochemical systems as an economical and environmentally friendly substitute for traditional electrode materials.[14–16]

Whereas the feasibility of using biochar for the mentioned applications depends on the feedstock and pyrolysis conditions,[17] studies of the effect of pyrolysis conditions on medicinal *Cannabis sativa* biochar properties and its possible applications are lacking. This study analyses the impact of pyrolysis temperature on the physicochemical properties of *C. sativa* biochar and performs a preliminary evaluation of biochar produced at different temperatures as a soil amendment, electrode material, and contaminant adsorbent.

Experimental

Biochar production

Plants belonging to a variety of *Cannabis sativa* L. of chemotype II (same ratio between tetrahydrocannabinol (THC) and cannabidiol (CBD) cannabinoids) were grown under controlled conditions of light, humidity and temperature in a growth chamber. After harvesting inflorescences, branches and stems were dried and used as feedstock for biochar production. Stems were cut down to pieces of 2–3 cm and dehydrated at 105 °C for 24 hours. The resulting material was heated in a N_2 atmosphere at maximum temperatures of 400 (C-400), 600 (C-600) and 800 °C (C-800) for 60 minutes with a heating rate of 10 °C min^{-1} in a tube furnace (Indef Model T-300). A cooling rate of 5 °C min^{-1} was maintained until a temperature of 25 °C was reached. Both heating rate and selected pyrolysis time are values typically used in the pyrolysis process. Mass yield (%) was calculated from the weight lost in each pyrolysis process ($N = 2$).

Physicochemical characterization

Surface area. BET area measurements were performed using a Micromeritics FlowSorb II 2300. Biochar of each temperature was ground with a mortar and its surface area was measured based on the gas adsorption method (Micromeritics FlowSorb II 2300).

Wettability. To analyse the hydrophobicity of the material, water contact angles were determined in three different samples of C-400, C-600 and C-800. A 3 μL bidistilled water drop was deposited on the longitudinal surfaces of each biochar sample and contact angles were measured using a goniometer (RAME HART) during the time until the drop was adsorbed. The initial contact angle (2 seconds since deposition on the surface) was registered.

pH and water holding capacity. Biochar pH was measured in triplicate in bidistilled water (pH 7.52) and 1 M KCl solution (pH 7.49) in a 1 : 10 proportion (w/v) with a pH meter (Sper Scientific)

after 1 hour of shaking and 1 hour of stabilization at 24 °C. ΔpH was also determined as described by Al-Wabel *et al.*[32] as an indirect indicator of net charge of the material surface.

The water-holding capacity (WHC) measurement of biochar was adapted from the literature.[23] Firstly, cellulose filters (maximum aperture 22 μm) were dried for 1 hour at 105 °C. An amount of 1 g of each biochar was mixed with 10 mL of deionized water and incubated at 25 °C for 7 days, this was carried out in triplicate. After that, the solutions were passed through the filters in a funnel until the water stopped dripping down. The water-saturated biochar samples with filters were weighed and then dried overnight at 105 °C. Finally, the dried filters containing biochar were weighed again. The WHC of biochar was calculated using the equation proposed by Zhang *et al.*[23]

SEM observation, EDS analysis and pore measurements. Transversal and longitudinal cuts of biochar included in epoxy resin were metallized with gold and observed by Scanning Electron Microscopy (SEM). Images were taken at different magnifications and Energy-Dispersive Spectroscopy (EDS) was also performed at random spots of two different samples to identify the elemental composition of each sample. Pore diameter was measured using IMAGEJ software from images taken by SEM.

FTIR spectroscopy. Fourier Transformed IR spectroscopy was performed on dried samples with Nicolet 6700 (Thermo Scientific) equipment.

RAMAN spectroscopy. Raman spectra were acquired in a Renishaw InVia reflex system equipped with a charge-coupled device (CCD) detector of 1040×256 pixels. A 514 nm diode laser (50 mW) was used as an excitation source in combination with a grating of 2400 grooves mm^{-1} and slit openings of 65 μm, which yield a spectral resolution of about 4 cm^{-1}. The laser power was kept to 100%. A $50\times$ (0.5 NA) long working distance (8 mm) Leica metallurgical objective was used in the excitation and collection paths. Spectra were typically acquired in 10 seconds with 2 accumulations.

TGA. Thermogravimetric assays (TGA) were performed on cannabis feedstocks that were heated under an anoxic atmosphere simulating pyrolysis conditions at maximum temperatures of 400, 600 and 800 °C. Biochar samples C-400, C-600 and C-800 were heated under an oxygenic atmosphere and the maximum temperature of 750 °C was maintained for 60 minutes. In both assays the heating rate was set as 10 °C min^{-1}. Evolution of sample weight and the derivative of weight change were reported.

Ash content. Ash content was measured following a standard procedure. Ceramic crucibles were placed in a muffle furnace at 600 °C for 2 hours. Approximately 1 g of biochar dried at 105 °C overnight was placed in the crucibles. The crucibles with the biochar were placed in a muffle furnace and heated at 600 °C for 4 hours to ensure complete combustion of organic matter. After cooling to room temperature in a desiccator, the crucibles were weighed again. The ash content was calculated as the ratio of the residue weight to the initial sample weight, expressed as a percentage. All measurements were performed in triplicate.

Electrical conductivity. The electrical conductivity of biochar produced at different temperatures was measured using a 2-point cell according to Antic Gorrazzi *et al.*[14] A power source applied potential differences to the material while current flow was recorded. The resulting current against potential difference plot yielded a straight line, with the slope indicating conductance (the inverse of resistance). Conductivity was calculated by multiplying conductance by the material's length and dividing by its cross-sectional area. Measurements were performed in duplicate for each temperature of biochar.

Zeta potential. Biochar samples were ground in a manual pulverizing mill in a tungsten carbide vessel (HSM, Herzog). Two cycles of 30 seconds each were performed. Then, the particle size distribution was analysed by laser diffractometry (Cilas 1190 particle size analyser) to confirm that particles with a size distribution smaller than 10 mm were obtained. The samples were resuspended in a high (100 mM) and a low (10 mM) salt solution (KNO_3), sonicated in a water bath for 20 minutes and stored for 24 hours to stabilize the pH. Samples were sonicated again for 20 minutes, and the pH was measured (it was around 5.5 for each sample). The pH was lowered with HNO_3 (pH 3) or increased with KOH (pH 13). Zeta Potential (ZP) was measured immediately after pH adjustment. ZP is shown as the mean of three measurements (100 runs each). Three independent analyses were performed.

Cannabis biochar applications

Plant growth assay. Tomato (*Solanum lycopersicum* cv. Platense) was the species selected to evaluate the effect of cannabis biochar on germination and plant growth. Tomato seed surface was sterilized in 30% (by volume) hypochlorite solution for 15 minutes followed by three washings with sterilized distilled water. After sterilization, seeds were placed in plastic pots containing a commercial substrate, supplemented 5% (w/w) with cannabis biochar obtained at different temperatures (400, 600 and 800 °C). A control treatment was also conducted using the substrate without biochar supplementation. Twelve plants were used for each treatment and two independent experiments were performed. Plants were grown for 18 days at 25 °C, under 250 μmol photons m^2 per s with a 16 : 8 hours light : dark cycle. Germination percentage was measured, and the height of the seedlings was recorded periodically throughout the duration of the experiment.

Adsorption assay. The ammonium adsorption capacity of cannabis biochar was evaluated on tubes containing 40 mL of solutions with 0, 5, 10, 50, 100, or 200 mg NH_4^+-N L^{-1}. Cannabis biochar produced at 400 and 800 °C was dried at 105 °C for 2 hours. After that, biochar was added to reach a concentration of 12.5 g L^{-1} in each tube. A control without biochar was carried out for each concentration. All tubes were shaken overnight at 150 rpm, in darkness at 20 °C.

Finally, NH_4^+-N L^{-1} was measured with an ammonia ion selective electrode (HANNA HI 4101) following the procedure provided by the manufacturer. Adsorption data were fitted to Langmuir (eqn (1)) and Freundlich (eqn (2)) isotherm models:

$$q_e = \frac{Q_0 k_L C_e}{1 + k_L C_e} \tag{1}$$

$$q_e = k_f C_e^{\frac{1}{n}} \tag{2}$$

where q_e is the adsorbed ammonia (mg NH_4^+ L^{-1}), Q_0 (mg NH_4^+ L^{-1}) is the maximum sorption capacity, k_L (L mg^{-1}) is the Langmuir constant, C_e (mg NH_4^+ L^{-1}) is the equilibrium concentration in the liquid medium after the adsorption, $1/n$ (dimensionless) is a parameter of Freundlich equation referring to the intensity and affinity for adsorption and k_f (mg$^{1-1/n}$ L$^{1/n}$ g^{-1}) is the Freundlich adsorption constant. The data were fitted to these equations using the genfit function in Mathcad® software.

Biochar as an electrode material. Cannabis biochar samples of three different temperatures (400, 600 and 800 °C) were tested as working electrode materials in a three-electrode electrochemical cell. Portions of each cannabis biochar were embedded in epoxy resin, leaving a cross-sectional area of the material exposed. Photographs were taken and digitally analysed to determine the resulting geometric electrode area which was used to calculate current density. To test the biochar electrodes for electrochemical reactions, cyclic voltammetries (CVs) were performed at different scan rates in a solution with 50 mM of ferricyanide redox compound and 0.5 M KCl. The reference electrode was Ag/AgCl 3 M NaCl and a platinum wire was the counter-electrode. The assay was performed in triplicate for each tested biochar. CVs were repeated using graphite rods as the working electrode. Due to the high electrolyte concentration, no solution resistance compensation was applied on the CVs.

The electrodes were also tested as anodes for the growth of electro-active bacteria. An inoculum of *Geobacter sulfurreducens* strain DSM12127 was added to the three-electrode cell (to reach 1×10^6 to 1×10^7 bacteria per cm^3 final concentration) that contained deoxygenated culture medium commonly used for this bacterium with acetate (20 mM) as the electron donor and no fumarate (electron acceptor). The culture medium was circulated with the electrochemical cell using PharMed tubing and a low-rate peristaltic pump. The pH of the medium was kept constant at a value of 7.3 by bubbling all media reservoirs and the reactor with a mixture of N_2 : CO_2 (80 : 20). Working electrodes of C-800 and graphite were polarized at a constant potential of 0.2 V *vs.* an Ag/AgCl (3 M NaCl) reference electrode by using a Pt wire as a counter electrode and the evolution of the current density was evaluated to monitor the growth of the electroactive bacteria. CVs were performed prior to inoculation and once a stable current density was achieved.

All electrochemical assays were performed by using an AUTOLAB PGSTAT101 potentiostat controlled by 2.1 NOVA dedicated software.

Statistical analysis

All results were first tested for normality and homoscedasticity. Differences between treatments and the control were evaluated using a one-way analysis of variance (ANOVA). Tukey's test was

used for *post hoc* comparisons. Data are reported as mean ± standard deviation. Differences were considered statistically significant when p value < 0.1. All statistical analyses were performed using R software.

Results and discussion

Physical and chemical properties of cannabis biochar and pyrolysis temperature effects

One of the main parameters affecting biochar physicochemical properties is the feedstock composition and structure. *C. sativa* stems cultivated for therapeutic purposes are composed of 77% holocellulose and 4–5% lignin[18] turning it into a cellulose-rich, non-woody, biomass. Besides this, the composition strongly varies between tissues. Xylem fibers have a high lignin content, whereas phloem fibers are primarily composed of cellulose. Other components in cell walls include hemicelluloses (4%), pectins (4%), proteins (3%), and trace of phenolic acids (<0.01%).[19] Stems of *C. sativa* exhibit a basipetal gradient of lignification, with the older, basal sections displaying a more developed xylem structure. The physicochemical and biological attributes of cell walls are influenced by various factors, like genotype, environmental conditions, and/or management.[19]

Although biochar obtained at different temperatures preserved the original structure of *C. sativa* stems (Fig. 1), the composition and physicochemical properties of biochar are determined by the peak pyrolysis temperature which governs the thermochemical transformations undergone by the feedstock.

These transformations can be monitored through thermogravimetric analysis (Fig. S1, ESI†). At temperatures up to 200 °C a weight loss corresponding to material dehydration is observed. During this first stage, light volatile compounds also evolve whereas hydroperoxide –COOH and –CO groups are formed.[17] Accompanying the increment in temperature from 200 to 500 °C, cellulose and hemi-cellulose decompose to simpler structures while gaseous products, including CO, CO_2, CH_4, and a bio-oil are formed with its production increasing with pyrolysis temperature.[20] These chemical modifications lead to a mass yield of around 30% for cannabis feedstock (Table 1).

For temperatures above 500 °C, although no significant weight variations are observed in TGA analysis, the biochar structure is subjected to considerable transformations. For instance, lignin undergoes transformations similar to those of cellulose above this temperature.[21] Consequently, as the pyrolysis temperature increases, biochar develops a progressively more ordered carbon structure that impacts its physicochemical properties.[17]

A surface area increment with pyrolysis temperature is also observed (Table 1) as volatilization of organic matter leads to the formation of micropores, vascular bundles or channel structures.[17] Despite this increment, all cannabis biochar showed a relatively low surface area compared to biochar obtained from other feedstocks, for example, 25.8 $m^2 g^{-1}$ for coconut shell, 185.6 $m^2 g^{-1}$ for sugarcane and 154.7 $m^2 g^{-1}$ for rice husks.[17] This low area may be probably due to the low lignin content of the feedstock and relatively high ash.[17,22] Also, a low water holding capacity compared to other biochars was observed, which could be associated with the low surface area of the material.[23]

The ash content of a biochar refers to the amount of non-combustible inorganic material that remains after the complete combustion of the biochar. EDS analysis identified Na, K and Ca as the principal constituent elements of the mineral phase (Table S2, ESI†). An increase in the ash content of cannabis biochar with rising temperature was observed (Table 1) which occurs because minerals remain in the solid phase during pyrolysis while oxygen, hydrogen and carbon are partially released as gaseous compounds.

Due to the presence of salts of alkali and alkaline elements like Na, K and Ca and the high ash content, cannabis biochar has a high pH, around 10 (Table 1), as reported for other biochars.[17,24]

Properties affecting adsorption and bacterial adhesion

The physicochemical properties of a solid surface play a critical role in the adhesion of particles and microorganisms. Hydrophobicity affects the interactions between the biochar surface and water. Whereas a highly hydrophobic surface repels water molecules, enhancing the adsorption of nonpolar compounds such as oils, greases and hydrophobic microbial cells, conversely, lower hydrophobicity favours interactions with polar substances. Cannabis biochar proved to be hydrophilic (contact angles < 90° as shown in Table 1) and its hydrophilicity increased along with pyrolysis temperature. Cellulose, unlike lignin, is a hydrophilic compound. Thus, cellulose-rich biomass, such as cannabis stems, produces hydrophilic biochar. The slight increment of hydrophilicity with temperature is
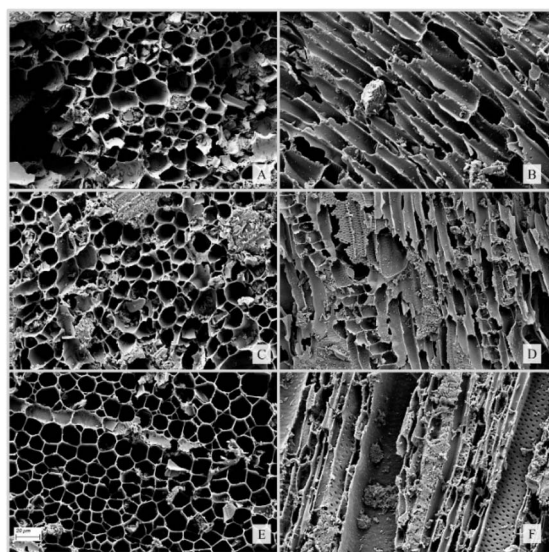

Fig. 1 SEM images of *Cannabis sativa* L. chemotype II stem-derived biochar produced at 400 °C (A and B), 600 °C (C and D), and 800 °C (E and F). Cross-sectional views are displayed on the left side, while longitudinal sections are shown on the right side.

Table 1 Physicochemical properties of cannabis biochar obtained at 400 °C (C-400), 600 °C (C-600) and 800 °C (C-800)[a]

Biochar	Mass yield (%)	SA (m² g⁻¹)	Ash (%)	θ_{water}	pH_{water}	WHC (g g⁻¹)	σ (S cm⁻¹)	ZP^b (mV)
C-400	32.18 ± 0.76	9	18.05 ± 0.15	66.05 ± 3.29	10.5 ± 0.02	2.18 ± 0.11	$1.63 \times 10^{-7} \pm 3.38 \times 10^{-8}$	-53.43 ± 7.69
C-600	29.03 ± 3.92	8.1	22.90 ± 2.51	44.03 ± 4.09	10.36 ± 0.02	1.88 ± 0.05	0.004 ± 0.003	-58.7 ± 6.19
C-800	27.06 ± 0.5	14.9	23.86 ± 2.19	37.46 ± 9.88	10.51 ± 0.02	2.09 ± 0.23	0.214 ± 0.013	56.20 ± 6.83

[a] SA: specific area, θ_{water}: contact angle in water, WHC: water holding capacity, σ: electrical conductivity, ZP: zeta potential. [b] At pH 7 and 10 mM KNO_3.

associated with an increase in surface area.[23] The hydrophilicity may impair the adhesion of bacterial cells that have a hydrophobic external membrane[25] but may favour the adsorption of polar compounds.[26]

Additionally, surface charge, commonly assessed through zeta potential, influences electrostatic interactions with charged particles and microorganisms, affecting adsorption and aggregation processes. Zeta potential is a measure of the indirect surface charge of a particle[27] and stability in solution. ZP values of cannabis biochar indicate a constant negative surface charge with increasing pyrolysis temperature (Table 1). This negative surface charge is also observed in ΔpH measurement with no differences between temperatures (Table S1, ESI†).

Although its negative charge is not particularly high, it can inhibit the adhesion of microorganisms which are, typically, negatively charged. Conversely, it may enhance the adsorption of positively charged particles and compounds, potentially hindering contaminant removal while simultaneously facilitating interactions between microorganisms and biochar through the adsorbed compounds.

Cannabis biochar as a soil amendment for plant growth

To assess the effect of cannabis biochar as a soil amendment and determine the optimal pyrolysis temperature for this application, the performance on tomato crop growth was evaluated.

Seed germination begins with imbibition and represents one of the most critical stages in plant development, as it significantly influences subsequent growth and overall crop yield.[28] As the cost of the substrates that provide optimal conditions for germination has risen, assessing this parameter has become increasingly important. Furthermore, obtaining natural supplements that enhance crop growth can also be of great importance for avoiding soil contamination and indirect CO_2 emissions caused by the excessive use of chemical fertilizers.

Effects of biochar as a soil amendment depends on the source material and pyrolysis temperature. Whereas reduction in germination was observed in other studies with biochar obtained from red cedar,[29] trunks of poplar trees,[30] and rice straw and wood sawdust,[31] cannabis biochar has proved to be biocompatible in germination assays (Fig. 2). Therefore, cannabis biochar stands out as a suitable choice for enhancing soil quality. The germination percentage of tomato seed remained constant with the soil supplemented with C-400 and C-800 compared to the control. However, a significant decrease in germination percentage was observed with C-600 biochar.

Since germination is a biological process strongly related to water availability, these results align with the higher surface area and water retention capacity observed in C-400 and C-800, compared to C-600 (Table 1).

In terms of plant growth, substrates supplemented with C-800 and C-600 did not show significant differences compared to the control treatment (Fig. 2). The best results were observed with C-400, which exhibited a significant increase in this parameter compared to the control and C-600 treatment.

As shown above, at low temperatures (between 350 °C and 500 °C), cannabis biochar structure contains compounds such as quinol and other aromatic groups (Fig. S2†). These compounds can be used as electron donors or acceptors for bacteria in soil[32] enabling biochar to enhance microbial growth and activity. In addition, the physicochemical properties of biochar can affect nutrient availability (Ca^{2+}, K^+, Mg^{2+}, PO_4^{3-}, NH_4^+), enhance water retention, and regulate pH in the soil, contributing to improving structure and fertility.[8] A more detailed analysis of the influence of cannabis biochar on rhizome microbial composition, as well as nutrient availability and its use by plants, is needed to better comprehend the reasons behind the observed increase in plant growth.
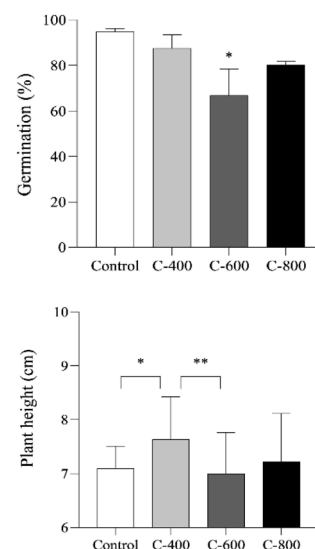

Fig. 2 Germination percentage (up) and height (down) of tomato plants grown in soil supplemented with different biochar samples. Data are expressed as the mean values $\pm$ SD. Standard deviation values range between 5 and 12% of the mean in all cases (note that the y-axis scale starts at 6 cm). Significant differences between conditions are shown with asterisks.

Ammonium adsorption

Biochar is widely used for the adsorption of contaminants from water, wastewater and soil due to its large surface area, high porosity, relatively low cost, and minimal environmental impact. In this study, the ammonia adsorption capacity of biochars produced at different pyrolysis temperatures was quantified. Ammonia was selected because in addition to its role in surface water contamination and eutrophication when discharged in wastewater, it is also a key component of fertilizers.

A significant portion of ammonia from fertilizers is often lost from fields through leaching, which not only has economic implications for agricultural production but also contributes to the pollution of ground and surface waters. In this context, biochar, through its surface adsorption properties, could enhance nitrogen retention in soil, thereby improving the efficiency of applied fertilizers and reducing water contamination. Ammonium retention by biochar can be explained by electrostatic adsorption to negatively charged oxygen-containing surface functional groups.[33]

In accordance with this, biochar obtained at lower temperatures, which as shown earlier has higher content of quinones (Fig. S2†) and O/C ratio (Table S1, ESI†), has a higher ammonia adsorption capacity. Maximum adsorption capacities estimated with the Langmuir isotherm (Fig. 3) were $Q_0 = 32.6$ mg NH_4 L^{-1} for C-400 and $Q_0 = 7.1$ mg NH_4 L^{-1} for C-800. With Freundlich isotherm a worse fitting was obtained ($R^2 = 0.947$ for C-400 and $R^2 = 0.921$ for C-800 as shown in Fig. S5, ESI†). The adsorption capacity of C-400 is much higher than that obtained for other biochars, even when subjected to chemical pretreatments for maximizing its adsorption capacity (6.4 mg NH_4 L^{-1} for maple biochar oxidized with H_2O_2),[33] indicating that cannabis biochar is a suitable option as an ammonia adsorbent in wastewater treatment and in soil applications. Experiments were also performed with C-600 biochar; however, presumably due to heterogeneities in its chemical composition, this material exhibited inconsistent performance. As a result, the obtained data were not clear enough to draw reliable conclusions about its behaviour.

Cannabis biochar as an electrode material

When biochar is obtained at high temperatures, carbon compounds crystallize into an ordered graphite structure,
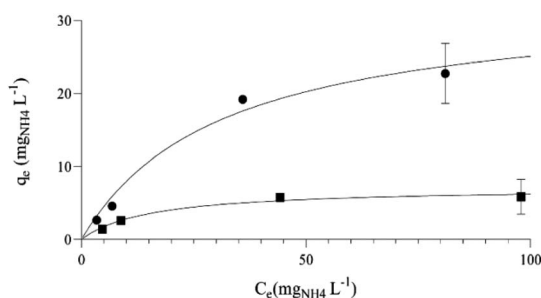
Fig. 3 Ammonia adsorption isotherms for C-400 (circles) and C-800 (squares). The fitting lines correspond to the Langmuir isotherm (with $Q_0 = 32.6$ mg$_{NH4}$ L^{-1}, $k_L = 0.032$ L mg$_{NH4}$$^{-1}$, $R^2 = 0.986$ for C-400 and $Q_0 = 7.1$ mg$_{NH4}$ L^{-1}, $k_L = 0.065$ L mg$_{NH4}$$^{-1}$, $R^2 = 0.984$, for C-800).

imparting electrical conductivity to the material.[14] In accordance with this graphitization (Fig. S4†), the electrical conductivity of biochar increased with pyrolysis temperature (Table 1).

Electrical conductivity measured on C-800 is lower but in the order of that measured for graphite (0.884 ± 0.19 S cm^{-1}). Graphite is widely used as an electrode material in various applications, including batteries, fuel cells, and bio-electrochemical systems where bacteria catalyse oxidation or reduction reactions. However, the production of graphite electrodes requires mining and energy-intensive beneficiation and purification processes, leading to a significant environmental impact.[34] Due to these factors and its relatively high cost, alternative electrode materials are being developed.

With the aim of testing cannabis biochar produced at different pyrolysis temperatures as an electrode material, we assembled electrodes made of pyrolyzed cannabis stem and used it as a working electrode in a three-electrode electrochemical system (see the Experimental section for details). The performance of biochar electrodes was tested and compared with graphite electrodes in a typical redox reaction and in their application as anodes for the growth of *G. sulfurreducens*, a model electro-active bacterium widely applied in bio-electrochemical systems.

Electrochemical response

The electrochemical response of the electrodes was analysed through cyclic voltammetry in a solution with ferricyanide. Ferricyanide and ferrocyanide are commonly used to study electrode materials in electrochemical systems because of their well-known redox behaviour and reproducibility. Voltammograms obtained with graphite, C-600 and C-800 electrodes at different scan rates are shown in Fig. 4.

Due to the low conductivity of the biochar obtained at lower temperatures, no signal was observed for electrodes made from C-400 (data not shown). However, for electrodes made from biochar obtained at higher temperatures, the voltammetric signal progressively improved. On the C-600 electrode the reduction of ferricyanide and subsequent oxidation of ferrocyanide, its reduction product, could be observed. Nevertheless, due to the low electrical conductivity of the electrode, the voltammetric signal was relatively weak. The flow of current through the low-conductivity electrode induces a potential drop, thereby requiring the application of higher potentials for oxidation reactions and lower potentials for reduction reactions. Consequently, in the voltammetric signal, the current peaks are shifted, and the peak separation is larger compared to that observed on more conductive electrodes such as graphite.

On the other hand, the voltammetric response of C-800 electrodes closely resembles that of graphite, suggesting that this biochar could be a suitable electrode material.

Kinetic constants for ferrocyanide reduction on C-800 and graphite electrodes were obtained through the widely applied Nicholson method.[35,36] The value for C-800 was $7.78 \times 10^{-4} \pm 1.22 \times 10^{-4}$ cm s^{-1} while for graphite electrodes the obtained value was $5.38 \times 10^{-4} \pm 0.22 \times 10^{-4}$ cm s^{-1}, which agree with
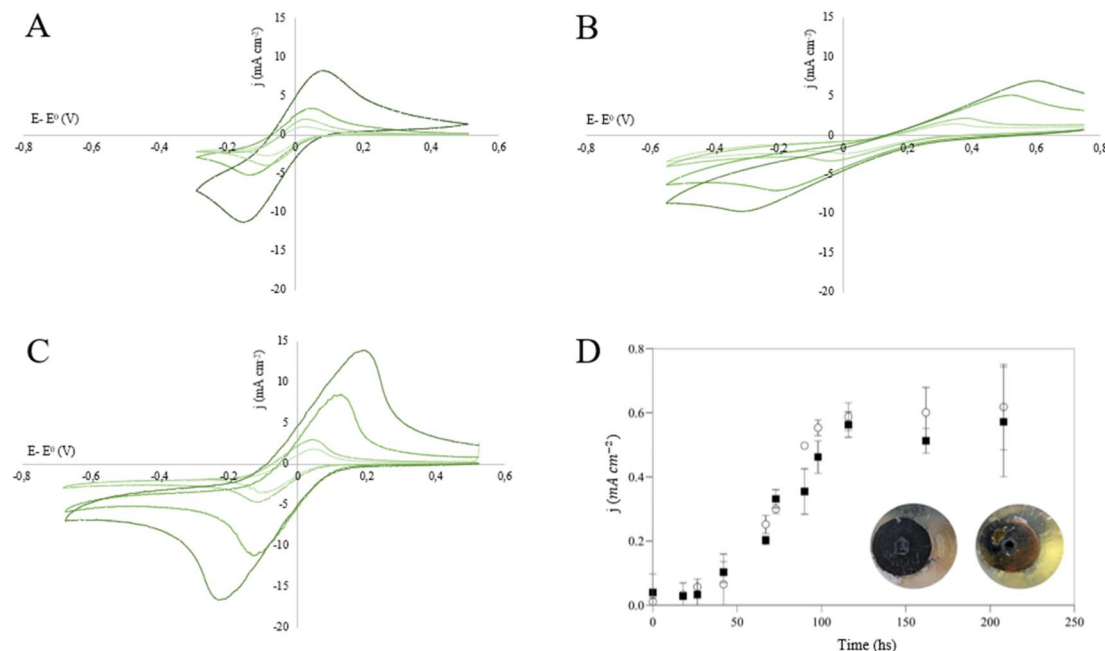
Fig. 4 (A–C) Cyclic voltammetry at 5, 10, 50 and 100 mV s^{-1} (in crescent tone from light to dark green, correspondingly) on ferricyanide solution with electrodes made of graphite (A), C-600 (B) and C-800 (C), a colour version of the manuscript can be found online. (D) Evolution of current density produced by *G. sulfurreducens* on graphite (open circles) and C-800 (squares) anodes polarized at 0.2 V (*vs.* Ag/AgCl). Inset: images of C-800 electrodes before (left) and after (right) the growth of *G. sulfurreducens*. Current density is expressed relative to the geometric area of the electrodes in all cases.

the kinetic constant reported for other carbonaceous electrodes.[37] The capacitance of C-800 biochar was obtained from cyclic voltammetries performed in a solution containing only the supporting electrolyte[38] (Fig. S7†), yielding a value of 0.0103 ± 0.001 F cm^{-2} (per unit of geometric area). This value is much higher than that of graphite electrodes (89 μF cm^{-2}) due to the roughness and internal porosity of the material.

Modeling of the C-800 electrode CVs was performed using an EC simulator.[39] A good fit to the experimental values was obtained with the mentioned kinetic constant but required a ferrocyanide diffusivity 1.6 times higher than the reported value for aqueous solutions. This may be attributed to the electrode roughness, which, according to previous reports, enhances mass transport to its surface.[40,41] More precise diffusivity and heterogeneous rate constant values could be obtained through a more detailed modeling of the electrochemical process, incorporating the effects of electrode surface roughness. However, this is beyond the scope of the present work, which aims to provide a qualitative comparison between biochar and graphite electrodes. In this regard, the fact that the estimated kinetic constants for C-800 and graphite electrodes are similar suggests that biochar electrodes are a suitable alternative to graphite for electrochemical applications.

Electro-active bacteria growth

Electro-active bacteria can use a polarized electrode as an electron donor or acceptor for its metabolic reactions, generating an electric current. They catalyse redox reactions on microbial electrochemical technologies (METs), which have

a wide range of applications that include wastewater treatment, biosensors and biosynthesis of high value products and energy carriers.

Due to its biocompatibility and high availability, graphite is the most common electrode material for the growth of these bacteria. Anyhow, the high cost of the electrodes represents a major drawback of METs and the development of efficient and cost-effective electrodes is a very active research field.[42]

As shown in Fig. 4D, *G. sulfurreducens* grows on C-800 electrodes at a similar rate to that on graphite electrodes, achieving similar stable current densities and forming a thick biofilm on the electrode surface (Fig. 4D, inset). This indicates that cannabis biochar electrodes may be suitable for replacing graphite in METs, thereby reducing the costs of such systems. Furthermore, the production of electrodes from both synthetic and natural graphite is energy-intensive and produces significant carbon emissions.[34] The production of biochar electrodes would require lower-cost equipment and lower energy input, and would be associated with a positive carbon footprint, thus reducing the environmental impact of METs.

Conclusions

This study successfully demonstrated the feasibility of converting cannabis residues into biochar, with various possible applications that depend on the physicochemical properties resulting from the peak pyrolysis temperature. Cannabis-derived biochar exhibits lower surface area and water-holding capacity compared to biochar produced from lignin-rich

feedstocks. However, low-temperature biochar (400 °C) demonstrated significant benefits for soil, enhancing tomato plant growth during early developmental stages. These effects are likely linked to the high content of quinones and related organic functional groups on the biochar surface. Further investigation is needed to fully understand the biological and physicochemical mechanisms driving these observations.

Additionally, the polar compounds on the surface of low-temperature biochar enhanced its ammonia adsorption capacity, outperforming high-temperature biochar (800 °C) and achieving higher adsorption capacities than those of biochars from other feedstocks. This high adsorption capacity not only enables the use of cannabis biochar for ammonia removal from wastewater but may also improve the efficiency of ammonia fertilization in soil by preventing its leaching.

On the other hand, at higher pyrolysis temperatures, the carbon structure undergoes graphitization, imparting electrical conductivity. This allows the use of cannabis biochar for electrochemical and bioelectrochemical reactions, achieving similar current densities to those with graphite electrodes, which are more expensive and have a higher environmental impact. The low cost and low environmental impact of biochar production makes high-temperature cannabis biochar a promising candidate for replacing graphite in electrochemical and bioelectrochemical systems.

Data availability

The data supporting this article have been included as part of the ESI.†

Author contributions

MBC and SAG: investigation, validation, data curation, formal analysis, visualisation and writing (original draft). SD and JM: methodology and investigation, validation and writing (review and editing). DN: funding acquisition, methodology, validation, supervision and writing (review and editing). SB: conceptualization, funding acquisition, investigation, project administration, methodology, supervision and writing (original draft).

Conflicts of interest

The authors declare no conflict of interest.

Acknowledgements

References

1 A. Seifalian, J. Kenyon and V. Khullar, *Int. J. Mol. Sci.*, 2022, **23**(24), 16201–16620.

2 A. C. Wartenberg, P. A. Holden, H. Bodwitch, P. Parker-Shames, T. Novotny, T. C. Harmon, S. C. Hart, M. Beutel, M. Gilmore, E. Hoh and V. Butsic, *Environ. Sci. Technol. Lett.*, 2021, **8**(2), 98–107.

3 K. Vávrová, O. Solcova, J. Knápek, J. Weger, K. Soukup, T. Humešová, T. Králík and J. Bím, *Fuel*, 2022, **329**, 125435.

4 J. Cui, X. Li, J. Lin, G. Guo, X. Zhang and G. Zeng, *Catena*, 2022, **214**, 106218.

5 N. Ullah, A. Ditta, A. Khalid, S. Mehmood, M. S. Rizwan, M. Ashraf, F. Mubeen, M. Imtiaz and M. M. Iqbal, *J. Soil Sci. Plant Nutr.*, 2020, **20**(2), 346–356.

6 S. Zhou, Z. Jiang, J. Shen, Q. Yao, X. Yang, X. Li, M. K. Awasthi and Z. Zhang, *Sci. Total Environ.*, 2023, **879**, 163067–163076.

7 X. Zhang, J. Song, W. Yan, T. Li, R. Li, J. Wang, X. Wang and Q. Zhou, *Sci. Total Environ.*, 2023, 855.

8 Y. Zhang, J. Wang and Y. Feng, *Catena*, 2021, 202.

9 L. Ye, M. Camps-Arbestain, Q. Shen, J. Lehmann, B. Singh and M. Sabir, *Soil Use Manag.*, 2020, **36**(1), 2–18.

10 A. Prado, R. Berenguer and A. Esteve-Núñez, *Carbon*, 2019, **146**, 597–609.

11 Y. Dai, N. Zhang, C. Xing, Q. Cui and Q. Sun, *Chemosphere*, 2019, **223**, 12–27.

12 N. Cheng, B. Wang, P. Wu, X. Lee, Y. Xing, M. Chen and B. Gao, *Environ. Pollut.*, 2021, **273**, 116448.

13 B. Qiu, X. Tao, H. Wang, W. Li, X. Ding and H. Chu, *J. Anal. Appl. Pyrolysis*, 2021, **155**, 105081.

14 S. Antic Gorrazzi, D. Massazza, A. Pedetta, L. Silva, B. Prados, G. Fouga and S. Bonanni, *RSC Sustain.*, 2023, **1**(5), 1200–1210.

15 P. Sangrulkar, S. Gupta and B. Kandasubramanian, *Bioresour. Technol. Rep.*, 2023, **24**, 101684.

16 N. N. Mohd Noor, K. Kim and K. Kim, *Fuel*, 2025, **381**, 133371.

17 A. Tomczyk, Z. Sokołowska and P. Boguta, *Rev. Environ. Sci. Biotechnol.*, 2020, **19**, 191–215.

18 K. K. Brar, Y. Raheja, B. S. Chadha, S. Magdouli, S. K. Brar, Y. H. Yang and A. Koubaa, *Biomass Convers. Biorefin.*, 2024, **14**(3), 3161–3182.

19 P. Amarasinghe, C. Pierre, M. Moussavi, A. Geremew, S. Woldesenbet and A. Weerasooriya, *Heliyon*, 2022, **8**(4), 9276–9287.

20 A. Escalante Rebolledo, G. Pérez López, C. Hidalgo Moreno, J. López Collado, J. Campo Alves, E. Valtierra Pacheco and J. D. Etchevers Barra, *Terra Latinoam.*, 2016, **34**(3), 367–382.

21 L. Marrot, K. Candelier, J. Valette, C. Lanvin, B. Horvat, L. Legan and D. B. DeVallance, *Waste Biomass Valorization*, 2022, 1–19.

22 S. Cui, F. Kong, Y. Li, Z. Jiang and M. Xi, *Sci. Total Environ.*, 2021, **779**, 146346.

23 Y. Zhang, B. Wang, M. Hassan and X. Zhang, *J. Environ. Manage.*, 2024, **370**, 122407.

24 B. Singh, B. P. Singh and A. L. Cowie, *Soil Res.*, 2010, **48**(7), 516–525.

25 C. Berne, C. K. Ellison, A. Ducret and Y. V. Brun, *Nat. Rev. Microbiol.*, 2018, **16**(10), 616–627.

26 A. M. Clurman, O. M. Rodríguez-Narvaez, A. Jayarathne, G. De Silva, M. I. Ranasinghe, A. Goonetilleke and E. R. Bandala, *Chem. Eng. J.*, 2020, **402**, 126277.

27 A. P. F. Maillard, J. C. Espeche, P. Maturana, A. C. Cutro and A. Hollmann, *Biochim. Biophys. Acta Biomembr.*, 2021, **1863**, 183597.

28 P. Carril, M. Ghorbani, S. Loppi and S. Celletti, *Plants*, 2023, **12**(12), 2235.

29 S. F. Vaughn, J. A. Byars, M. A. Jackson, S. C. Peterson and F. J. Eller, *Sci. Hortic.*, 2021, **280**, 109947.

30 X. Luo, Z. Wang, K. Meki, X. Wang, B. Liu, H. Zheng and F. Li, *J. Soils Sediments*, 2019, **19**, 3934–3944.

31 J. Zhang, J. Jin, M. Wang, R. Naidu, Y. Liu, Y. B. Man and S. Shan, *Environ. Res.*, 2020, **191**, 110034.

32 M. I. Al-Wabel, A. Al-Omran, A. H. El-Naggar, M. Nadeem and A. R. A. Usman, *Bioresour. Technol.*, 2013, **131**, 374–379.

33 B. Wang, J. Lehmann, K. Hanley, R. Hestrin and A. Enders, *Chemosphere*, 2015, **138**, 120–126.

34 D. Surovtseva, E. Crossin, R. Pell and L. Stamford, *J. Ind. Ecol.*, 2022, **26**(3), 964–979.

35 R. S. Nicholson, *Anal. Chem.*, 1965, **37**(11), 1351–1355.

36 M. G. Trachioti, A. C. Lazanas and M. I. Prodromidis, *Microchim. Acta*, 2023, **190**(7), 251.

37 M. A Buckingham, S. Hammoud, H. Li, C. J. Beale, J. T. Sengel and L. Aldous, *Sustain. Energy Fuels*, 2020, **4**(7), 3388–3399.

38 S. Trassatti and O. A. Petrii, *J. Electroanal. Chem.*, 1992, **327**, 353–376.

39 S. Wang, J. Wang and Y. Gao, *J. Chem. Educ.*, 2017, **94**(10), 1567–1570.

40 R. Kant, *J. Phys. Chem. C*, 2014, **118**(46), 26599–26612.

41 R. Kant, *Electrochim. Acta*, 2023, **111**, 223–233.

42 A. A. Mier, H. Olvera-Vargas, M. Mejía-Lopez, A. Longoria, L. Verea, P. J. Sebastian, *et al.*, *Chemosphere*, 2021, **283**, 131138.